Desalination and Water Treatment
www.deswater.com
doi: 10.1080/19443994.2013.832636

52 (2014) 7565–7574
December

Taylor & Francis
Taylor & Francis Group

Effect of ions on carbon steel corrosion in cooling systems with reclaimed wastewater as the alternative makeup water

Juntao Jin[a,b], Guangxue Wu[a,b], Kai He[a], Jun Chen[c], Guangming Xu[c], Yuntao Guan[a,b,*]

[a]*Research Center for Environmental Engineering and Management, Graduate School at Shenzhen, Tsinghua University, Shenzhen 518055, Guangdong, China*
[b]*State Environmental Protection Key Laboratory of Microorganism Application and Risk Control (MARC), Graduate School at Shenzhen, Tsinghua University, Shenzhen 518055, Guangdong, China*
Tel. +86 755 26036702; Fax: +86 755 26036511; email: guanyt@sz.tsinghua.edu.cn
[c]*Changzhou Drainage Administration, Changzhou 213077, Jiangsu, China*

Received 24 October 2012; Accepted 29 July 2013

ABSTRACT

The corrosion behavior of carbon steel in cooling systems using reclaimed wastewater as the makeup water was investigated. Effect of typical ions (Cl^-, SO_4^{2-}, NO_3^-, and NH_4^+) on the corrosion of carbon steel in cooling systems was evaluated. The electrochemical techniques such as potentiodynamic polarization and electrochemical impedance spectroscopy were used to measure the corrosion rate and analyze the corrosion processes. Also scanning electron microscopy, Fourier transform infrared spectrometer and energy dispersive spectroscopy were applied to surface analysis. Among the examined ions, Cl^- had the highest influence on the corrosion of the carbon steel, followed by SO_4^{2-}, NO_3^-, and NH_4^+. During cooling cycle, the corrosion process of carbon steel was controlled by cathodic reaction. Corrosion rate increased at the initial stage and then decreased thereafter due to the combined effect of ions and corrosion layer. The ions accelerated the initial corrosion of carbon steel in cooling system, while the corrosion layer hindered this effect. The corrosion layer was dense, uniform, and made up of crystalline particles and the main corrosion products were ferric hydroxides and iron oxide.

Keywords: Carbon steel; Reclaimed wastewater; Corrosion; Electrochemical methods; Ion influence

1. Introduction

With decreasing available water sources, reclamation of secondary treated wastewater is a promising water resource. The reclaimed wastewater can be used as either a substitute or augment of water sources, depending on the water quality requirement [1,2]. Many projects have been carried out using reclaimed wastewater as the makeup water for cooling systems, especially in the USA and Australia [3–5]. In steel industries, a huge volume of fresh water is required for cooling and boiler makeup. For example, more than 90% of the total water consumption in steel industries is by cooling system [6]. Due to its low water quality requirements, reclaimed wastewater can be used directly as cooling water in steel industries, resulting in reduced cost significantly.

*Corresponding author.

In cooling systems, the water constituents would be concentrated several times due to the evaporation of water. The elevated salt concentrations and high water temperature give rise to corrosion [7,8]. Especially, ions such as chloride (Cl^-) and sulfate (SO_4^{2-}) generally increase the corrosiveness of various metals [9]. In general, corrosion affected by ions is mainly induced by electrochemical processes. The presence of aggressive ions in reclaimed wastewater, such as Cl^-, sulfide (S^{2-}), or SO_4^{2-} has the potential to result in localized corrosion [10]. For example, the anodic dissolution of iron in chloride-containing solutions can be explained by the mechanism proposed by Tsuru [11]:

$$Fe + OH^- + Cl^- \leftrightarrow FeClOH^-(ads) + e^- \quad (1)$$

$$FeClOH^-(ads) \rightarrow FeOH^+ + Cl^- + e^- \quad (2)$$

$$FeOH^+ + H^+ \rightarrow Fe^{2+} + H_2O \quad (3)$$

The case of SO_4^{2-} can be attributed to the accelerating effect of HS^- ions through chemical or biochemical pathways, the prominent specie among the three forms of dissolved sulfur (H_2S, HS^- and S^{2-}). The anodic dissolution processes are as follows [12,13]:

$$SO_4^{2-} + 8H^+ + 8e \rightarrow HS^- + OH^- + 3H_2O \quad (4)$$

$$Fe + HS^- \leftrightarrow FeHS^-(ads) \quad (5)$$

$$FeHS^-(ads) \rightarrow FeHS^+(ads) + 2e^- \quad (6)$$

$$FeHS^+(ads) \rightarrow Fe^{2+} + HS^- \quad (7)$$

In addition, ammonia and nitrate are also the corrosive inducers for carbon steel in reclaimed wastewater. Ammonia is corrosive because it can form soluble substances with steel [14].

To avoid corrosion problems in cooling systems using reclaimed wastewater, it is necessary to investigate the effect of ions on the corrosion so as to better control this adverse effect. This study was aimed to examine the carbon steel corrosion in cooling systems using reclaimed wastewater as the makeup water and addressed the following aspects: influence of different ions on carbon steel corrosion in reclaimed wastewater, and carbon steel corrosion characteristics in cooling systems using reclaimed wastewater in a pilot-scale reactor.

2. Materials and methods

2.1. Effect of different ions on carbon steel corrosion

Effect of different ions on the corrosion of carbon steel was evaluated by the polarization measurement and weight loss. In order to evaluate the corrosion caused by different ions in reclaimed wastewater, deionized water (DI water) was selected and the pH of DI water was adjusted to seven with NaOH. Orthogonal experiment was carried out with ion concentration as shown in Table 1. The tested ion concentrations were within the range during the concentration cycle. After finishing the orthogonal experiment, the corrosion rate under different conditions was calculated by the weight loss of carbon steel. Besides the orthogonal experiment, the polarization experiment was carried out under different Cl^- and SO_4^{2-} concentrations of 2, 4, 6, and 8 mmol, respectively.

2.2. Simulated cooling system operation

The simulated cooling system is shown in Fig. 1 and the test pipe was made of carbon steel. The chemical composition of carbon steel was 0.17–0.23% of C, 0.17–0.37% of Si, 0.35–0.65% of Mn, ⩽0.035 of P, ⩽0.035 of S, ⩽0.30 of Ni, ⩽0.25 of Cr, ⩽0.25 of Cu, and all others of Fe. The size of test carbon steel pipe was 10 mm (diameter) × 1 mm(thickness) × 650 mm (length) for electrochemical measurement, 2 mm × 2 mm coupon samples for scanning electron microscopy (SEM) and energy dispersive spectroscopy (EDS), and 7.24 cm × 1.15 cm × 0.2 cm coupons for the weight loss measurement. For the simulated cooling system, the flow rate was 200 L/h, the inlet temperature was 28 ℃ (the same as the operational temperature in the selected steel work), and the concentration cycle was four.

The experiment was carried out for 16 days until the concentration cycle reached four. Cooling water was sampled on Days 0, 2, 4, 5, 7, 9, 11, 12, 13, 14, 15, and 16, and the electrochemical characteristics of water samples were detected by the polarization measurement and the electrochemical impedance spectros-

Table 1
The applied conditions used in the orthogonal experiment

Designed parameters	Cl^- (mg/L)	SO_4^{2-} (mg/L)	NO_3^- (mg/L)	NH_4^+ (mg/L)
Designed levels	100	100	20	1
	200	200	40	5
	300	300	60	10

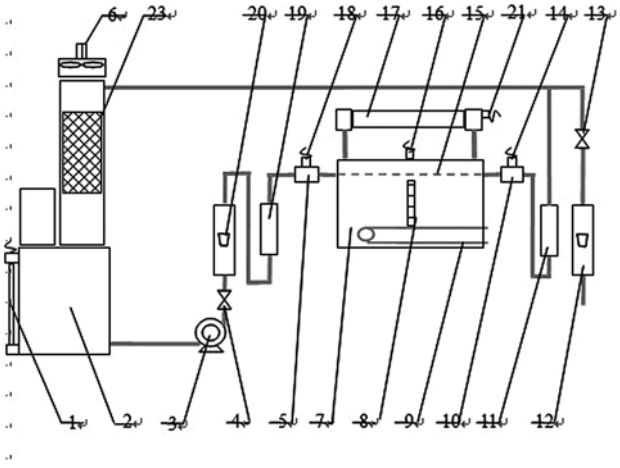

Fig. 1. Schematic diagram of the simulated cooling system. (1) Water level meter; (2) water tank; (3) circulating pump; (4) control valve; (5) inlet chamber; (6) fan; (7) steam generator; (8) water level meter in boiler; (9) electric heater; (10) outlet chamber; (11) specimen holder in outlet; (12) discharge flow meter; (13) discharge control valve; (14) outlet thermometer; (15) test pipe; (16) steam thermometer; (17) condensing plant; (18) inlet thermometer; (19) specimen holder in inlet; (20) flow meter; and (21) temperature sensor.

copy (EIS). In addition, dynamics of various ion concentrations was also evaluated during cycle.

2.3. Analytical methods

Gravimetric experiments (the precision was 0.01 mg) were carried out in a round glass with three nicks. The solution volume was 1 L. The initial weight of the specimen was recorded before immersion in the reclaimed wastewater. Temperature of the solution was maintained by thermostatically controlled water bath. The rotational speed of the specimens was set using a speed regulator motor (Motian, Jiangsu, China).

The corrosion rate (CR) of the carbon steel was determined after 72 h of immersion at various rotational speeds (70–90 rpm) at 50 °C using Eq. (8),

$$\mathrm{CR} = \frac{8,760 \times 10 \times W}{A\rho t} \tag{8}$$

where CR is the corrosion rate (mm/a), W is the weight loss (g), A is the area of the coupon (cm^2), ρ is the density of carbon steel (g/cm^3), and t is the immersion time (h).

Polarization measurements were performed by a CHI 660D electrochemical workstation at a 0.01 V/s scan step with a saturated calomel electrode as the reference and a platinum sheet as the counter electrode [15]. The scan range was +2 to −2 V. The carbon steel sample was used as the working electrode. The working electrode surface was covered with epoxy resin with an uncovered area of 0.4 cm^2.

The EIS measurement was carried out over the frequency range of 1 MHz–0.01 Hz with a 5 mV amplitude signal at an open circuit. Before all the electrochemical experiments were performed, the specimens were kept in the solution for 30 min in order to obtain a stable open-circuit potential [16]. All experiments were run in duplicates.

The components and morphology of corrosion deposits were determined by FTIR, EDS, and SEM. The structure and the composition of the corrosion scales were examined for carbon steel coupons placed in the circulating cooling water dynamic simulation system. The 2 mm × 2 mm samples were cut from the untreated corrosion coupons, which were examined by SEM for micrographs and EDS for element analysis on Days 0, 2, 5, 10, and 16. The corrosion products from coupons were removed from the surface, mixed with KBr powder, grinded, and then analyzed by FTIR.

3. Results and discussion

3.1. Physico-chemical characteristics of the cooling water

The reclaimed wastewater was taken from Qishuyan wastewater treatment plant in Changzhou, China. Characteristics of the reclaimed wastewater are shown in Table 2. No significant changes occurred in the concentrations of total alkalinity, SO_4^{2-}, Cl^-, and conductivity, which are the primary water quality parameters affecting metal corrosion

Table 2
Characteristics of reclaimed wastewater with average values for all parameters

Parameters	Unit	Reclaimed wastewater
pH	–	7.0 (6.95–7.14)
COD_{Cr}	mg/L	20.4 (10–22)
NH_4^+-N	mg/L	0.32 (0.24–0.4)
NO_3^--N	mg/L	9.7
Total phosphorus(TP)	mg/L	0.35 (0.15–0.37)
Cl^-	mg/L	66.2 (63–85)
SO_4^{2-}	mg/L	94.5 (64–101)
Total alkalinity	mg $CaCO_3$/L	138 (85–141)
Total hardness	mg $CaCO_3$/L	180 (179–220)
Total iron	mg/L	0.04
Conductivity	μS/cm	534 (526–542)
LI	–	1.35–3.37

[17–19]. The total alkalinity varied from 85 to 141 mg/L, SO_4^{2-} was in range of 64–101 mg/L, and Cl^- was found with concentrations ranging from 63 to 85 mg/L. The conductivity value was in the range of 526–542 μS/cm. Meanwhile, the Larson–Skold Index (LI) ($[Cl^-]+2[SO_4^{2-}]/[HCO_3^-]$) was used as a predictive measurement of iron corrosion [20,21], high corrosion rates occur at LI > 1.2. In the study, LI was calculated as 1.35–3.37, with a high corrosion potential for the carbon steel.

3.2. Effects of different ions on corrosion in the cooling system

The effect of Cl^-, SO_4^{2-}, NO_3^-, and NH_4^+ on the corrosion rate was examined with the orthogonal design of $L_9(3^4)$. The corrosion was influenced sequentially by Cl^-, SO_4^{2-}, NH_4^+, and NO_3^- (Table 3). The corrosion rate of carbon steel was accelerated with increasing ion concentrations by the order of $Cl^- > SO_4^{2-} > NH_4^+ > NO_3^-$. It could be attributed to the anionic infiltrability size, which determined the ability to destroy metal protective film. The larger the seepage failure effect, the higher the corrosion rate [22]. Cl^- not only has the largest anionic infiltrability size, but also accelerates anodic dissolution as described above.

Besides acting as a corrosive medium and catalyzing the penetration of oxygen into steels, SO_4^{2-} can cause the production of sulfate-reducing bacteria (SRB), the organisms most closely identified with microbiologically influenced corrosion (MIC). They are a group of ubiquitous, diverse anaerobes that use sulfate ions as terminal electron acceptor. Several mechanisms have been attributed to SRB, including cathodic depolarization by the enzyme dehydrogenase, anodic depolarization [23], production of iron sulfides and its hydrolysis reaction, release of exopolymers capable of binding metal irons [24], sulfide-induced stress corrosion cracking, and hydrogen-induced cracking or blistering [25]. Because of the high concentration of DO, the growth of SRB was limited in the experiment. In the actual cooling system, the presence of oxygen gradients within the biofilm provides an anaerobic environment for SRB and the control of SRB become a boring problem in the inhibition of steel corrosion.

Nitrification of ammonia with the existence of high dissolved oxygen consumed alkalinity, resulting in a decrease of pH and enhancing carbon steel corrosion [26]. Moreover, accelerated disinfectant decay via nitrification could increase the growth of bacteria that might stimulate MIC [27]. The production of microbial product from nitrifier biomass might increase metal leaching via complexation with metal ions [28]. However, ammonia concentration in the reclaimed wastewater is low (0.24–0.4 mg/L) and its corrosion contribution is also very limited. The use of synthetic water in the orthogonal experiment was another likely reason why the nitrification process is limited and the role of ammonia was found not to be significant.

Based on the results from the above experiment, effect of Cl^- and SO_4^{2-} on carbon steel corrosion in the cooling system using reclaimed wastewater was further examined by the electrochemical analysis. Electrochemical parameters such as corrosion potential

Table 3
Corrosion rate from orthogonal experiment

	Cl^- (mg/L)	SO_4^{2-} (mg/L)	NO_3^- (mg/L)	NH_4^+ (mg/L)	Corrosion rate (mm/yr)
1	100	100	20	1	1.27
2	100	200	40	5	1.36
3	100	300	60	10	1.38
4	200	100	40	10	1.43
5	200	200	60	1	1.52
6	200	300	20	5	1.55
7	300	100	60	5	1.65
8	300	200	20	10	1.59
9	300	300	40	1	1.71
K1	1.339	1.452	1.473	1.503	
K2	1.504	1.493	1.505	1.524	
K3	1.653	1.552	1.518	1.470	
R	0.314	0.100	0.045	0.054	

Note: K1: the average of value in the first level, K2: the average of value in the second level, K3: the average of value in the third level, and R: range of levels.

(E_{corr}), polarization resistance, and corrosion current density (i_{corr}) were extracted by Tafel extrapolating the anodic and cathodic lines (Table 4). Under high Cl^- and SO_4^{2-} concentrations, the corrosion current density was high, showing a high corrosion rate of carbon steel. The corrosion current density increased and the polarization resistance decreased with increasing ion concentrations (until 6 mmol/L), ascribing to the infiltrability ability to metal protective film of ions accelerating anodic dissolution velocity [29]. Meanwhile, the infiltrability size of chloride is stronger than that of sulfate, so chloride has greater effect on the corrosion. Therefore, ions such as chloride and sulfate should be paid more attention to use reclaimed wastewater in cooling systems.

Effect of various ion concentrations on carbon steel corrosion to analyze their relationships was evaluated during cycling in the pilot-scale reactor and principal component analysis was used [30]. In this analysis, all the parameters were given the same weighting and preference function. Fig. 2 shows the dynamics of water quality and corrosion parameters in the cooling system (left) and relationships between them (right). As can be seen in Fig. 2, negative correlation occurred between SO_4^{2-}, Cl^-, and E_{corr} since variables in general agreements were oriented in the opposite direction in the GAIA plane, while NH_4^+ is slightly correlated on E_{corr}. This was of serious concern due to the difference with the results of the orthogonal test.

Table 4
Electrochemical parameters obtained from the polarization curves for carbon steel in reclaimed wastewater with various concentrations of Cl^- and SO_4^{2-}

Ion	Concentration	Corrosion potential (V)	Polarization resistance (Ω)	Corrosion current density (mA/cm^2)
	Reclaimed wastewater (RW)	−0.662	1146.2	0.1183
Cl^-	RW + 2 mmol/L	−0.666	790.7	0.1618
	RW + 4 mmol/L	−0.663	693.7	0.1812
	RW + 6 mmol/L	−0.621	388.9	0.3539
	RW + 8 mmol/L	−0.644	395.5	0.3231
SO_4^{2-}	RW + 2 mmol/L	−0.665	781.0	0.1537
	RW + 4 mmol/L	−0.679	744.6	0.1667
	RW + 6 mmol/L	−0.684	647.9	0.1829
	RW + 8 mmol/L	−0.671	451.0	0.2700

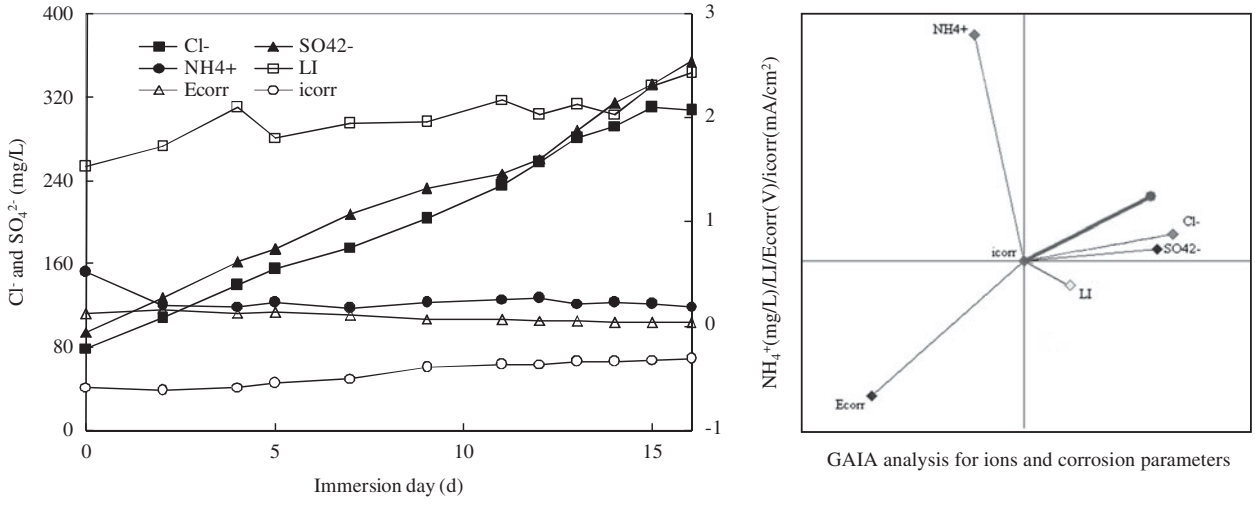

Fig. 2. Dynamics of water quality and corrosion parameters (E_{corr}, i_{corr}) in the cooling system with reclaimed wastewater as the makeup water (left) and GAIA analysis for ions and corrosion parameters (right).

3.3. Electrochemical behavior of corrosion

The potentiodynamic polarization curves for the carbon steel after 16 days of exposure in reclaimed wastewater for the cooling system are shown in Fig. 3. Values of the electrochemical corrosion parameters such as E_{corr}, i_{corr}, anodic Tafel slope (β_a), and cathodic Tafel slope (β_c) are presented in Table 5.

From the polarization plots, β_c was lower than β_a, which indicated that the corrosion of cathodic reaction (oxygen reduction) controlled the rate of the corrosion process [31]. β_c decreased and β_a increased with immersion time showing that the cathodic process was suppressed and the anodic reaction (iron dissolution) was accelerated. The reason was due to that corrosion products were produced on the steel surface and this hindered the diffusion of DO.

The corrosion potential, E_{corr}, underwent a negative shift of −39 mV on Day 2, and the corrosion current, i_{corr}, increased from 4.142 mA/cm^2 on Day 1 to 6.183 mA/cm^2 on Day 2, showing a higher electrochemical activity on the carbon steel surface affected by increasing concentrations of Cl^- and SO_4^{2-}. Furthermore, E_{corr} increased slowly to −0.316 V while i_{corr} decreased to 0.0303 mA/cm^2 on Day 16, indicating the formation of a corrosive layer supposedly protecting carbon steel from corrosion [32]. On the one hand, the corrosive layer hindered the diffusion of DO and the cathode reaction was restricted which matched with the initial conclusions of Tafel slope, on the other hand, the corrosive layer also reduced contact area of anion and carbon steel and weakened its corrosion effect on substrate.

Dynamics of the impedance behavior of carbon steel in reclaimed wastewater is presented in Fig. 4, which indicated that the impedance response of carbon steel changed significantly over time. The Nyquist plot could be divided into two semi-circles because of the formation of corrosion product layer on the metal surface [33]. The first semi-circle, which appeared at high frequencies, related to the response of the corrosion product layer. The difference among these plots was that the second semi-circle appeared at low frequencies. Indeed, the biofilm formation on the metal surface could show by another semicircle while the oxide layer on the steel surface had a diffusion characteristic and a diffusion tail appeared in the Nyquist plot. In the case of biofilm, we assumed that a strong interaction with metal always maintains the

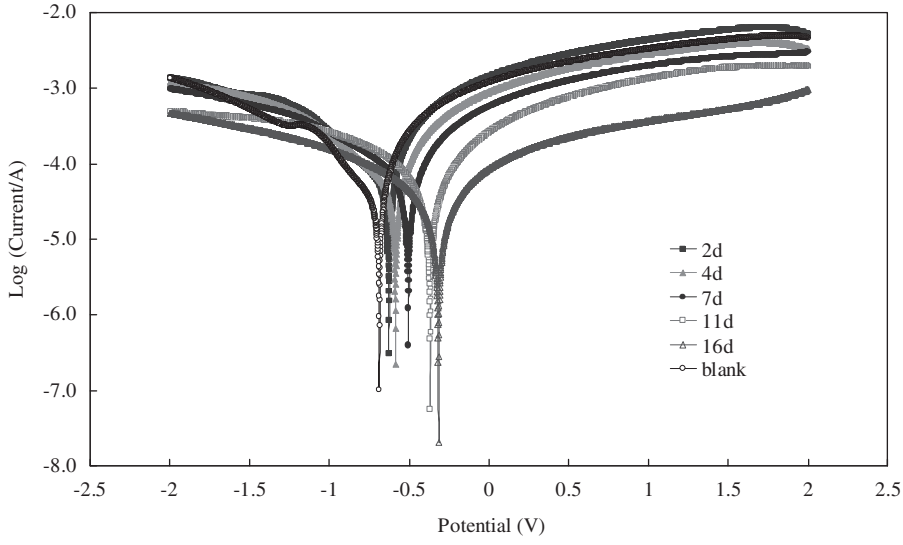

Fig. 3. Potentiodynamic polarization curve for carbon steel in reclaimed wastewater with various immersing time.

Table 5
Polarization parameters for carbon steel from the Tafel plots

	Blank	Day 2	Day 4	Day 7	Day 11	Day 16
Anodic Tafel slope β_a (V/dec)	3.123	4.223	3.196	4.106	4.718	4.799
Cathodic Tafel slope β_c (V/dec)	5.452	5.150	5.564	5.287	5.241	4.958
i_{corr} (μA)	6.205	14.02	4.598	3.811	2.315	1.15
E_{corr} (V)	−0.592	−0.602	−0.585	−0.502	−0.366	−0.316

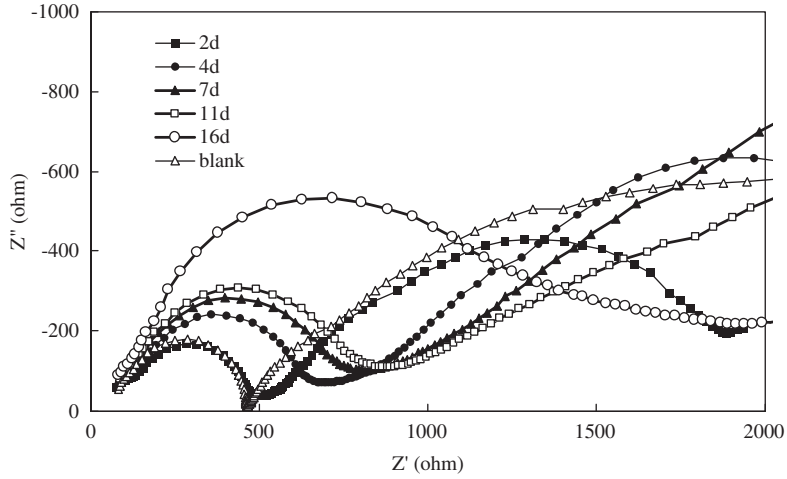

Fig. 4. Nyquist plots for carbon steel in reclaimed wastewater with various immersing time.

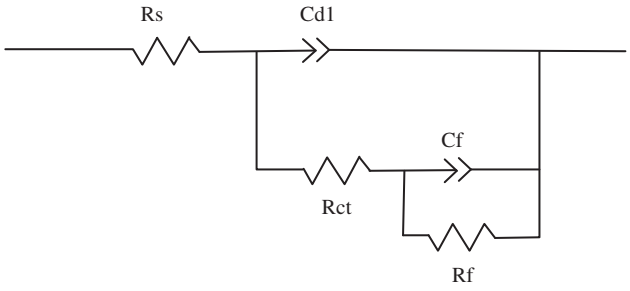

Fig. 5. Equivalent circuit proposed to simulate experimental impedance in the evaluation of carbon steel in cooling system.

surface active and accelerates anodic iron dissolution [34–36]. However, a direct description of the reaction process is not provided in this study.

To describe the impedance response of the corrosion phenomenon, an electric equivalent circuit involving a Warburg component namely R_{diff} and C_{diff} necessary for diffusion was used to model the experimental values (Fig. 5) and summarized in Table 6 [37]. As can be seen in Table 6, R_s values commonly associated with solution resistance varied within exposure time, which might be indicated by the existence of a small change in the composition of reclaimed water. The double layer capacitance (C_{dl}) increased on Day 2 and then decreased which suggested that changes occured in porosity and structure of the corrosion product layer and biofilm formed on the metal surfaces. The roughness of the surfaces was confirmed by parameter values and this interface exhibited a non-ideal behavior of the capacitor. Charge transfer resistance (R_{ct}) had lower values on Day 2 which suggested accelerated character of carbon steel oxidation process. R_{diff} and C_{diff} also showed the diffusion characteristics of oxide layer. R_{diff} showed that iron ions' (II or III) diffusion from the steel toward solution through the film of corrosion products was favored since the values of this resistance change as a function of immersion time in the system [38].

3.4. Structure and composition of the corrosion products

Fig. 6 shows the SEM micrographs of the corrosion scale on the carbon steel coupons taken on different days. The corrosion particles were loose on Day 2. On

Table 6
Electrical elements obtained from the best fitting of experimental impedance diagrams of the carbon steel, using ZSimDemo 3.30d program

	Blank	Day 2	Day 4	Day 7	Day 11	Day 16
R_s (kΩcm^2)	107.37	105	117.3	113.6	110.9	121.2
R_{ct} (kΩcm^2)	456.7	439.9	670.2	842.5	939.3	1,692
R_{diff} (kΩcm^2)	1,297	1,166	2025	2,387	2,486	2,877
$C_{dl} \times 10^{-9}$ F	5.14	7.53	7.15	5.02	4.37	4.25
$C_{diff} \times 10^{-5}$ F	4.04	1.51	9.14	6.24	7.24	7.60

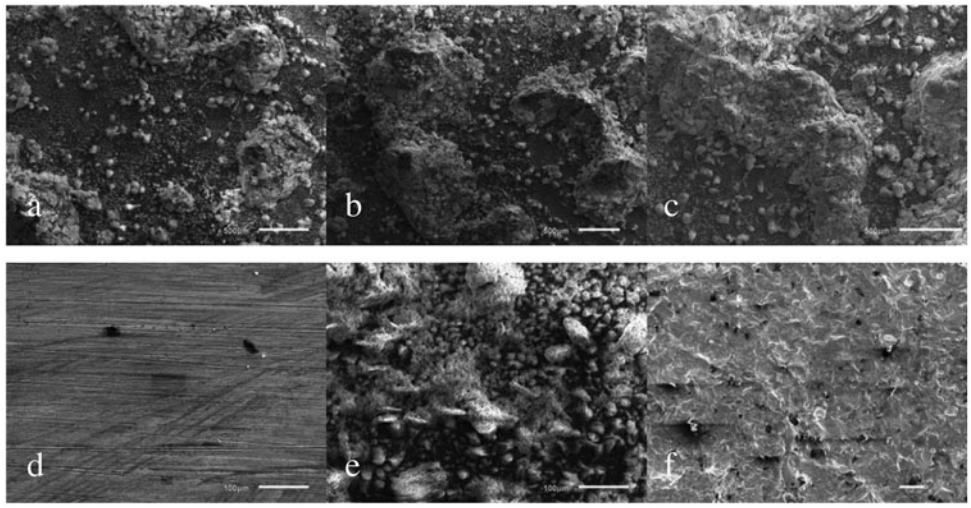

Fig. 6. Scanning electron microscopy (SEM) micrographs of the corrosion scales on the carbon steel coupons at different days. (a) Day 2; (b) Day 5; (c) Day 10; (d) Day 0; (e) Day 16 before cleaning; (f) Day 16 after cleaning.

Day 10, the morphology of scale surface was agglomerated and localized corrosion was apparent. Finally, the carbon steel was covered with dense, uniform, and good crystalline granular-particles. After removal of corrosion products, the surface seemed rough, which exhibited serious localized corrosion and etching pit. Furthermore, the elemental composition of three randomly selected scales was determined by EDS (Table 7). The content was 20–30% of ion and 48–54% of oxygen, indicating that the main component of the corrosion product was iron oxide. Iron oxide formation might be due to the high concentration of DO, which diffused and produced differential oxygen cells. These cells on the surface modified electrochemical processes and induced corrosion, especially when chloride concentration was high in reclaimed wastewater. The chloride destroyed carbon steel surface oxide layer, enhanced DO to react with carbon steel, and led to enhanced localized corrosion. A small amount of carbon (6%), calcium (8–13%), and phosphorus (0.3%) were also detected (Table 7). Carbon could be mainly formed from HCO_3^-, with the reactions as shown in Eqs. (9) and (10). Corrosion products contained Ca, P, and other elements, because iron oxide or iron hydroxyl oxide reacted with calcium phosphate easily and resulted in co-precipitation, forming a light yellow corrosive layer.

$$HCO_3^- \leftrightarrow H^+ + CO_3^{2-} \tag{9}$$

$$Fe^{2+} + CO_3^{2-} \rightarrow FeCO_3 \tag{10}$$

Fig. 7 shows the FITR pattern of the corrosion scale on carbon steel coupons. Ferric hydroxides (α-FeOOH and γ-FeOOH) and iron oxide (Fe_2O_3 and Fe_3O_4) were detected. The reason for ferric hydroxides formation was as follows: the forms of iron at pH 7 were $Fe(OH)_2$ and $Fe(OH)^+$, each about 50%. $Fe(OH)_2$ and $FeOH^+$ can be both transformed into

Table 7
The elemental composition ratio of corrosion products on three randomly selected scales measured by EDS

	Element								
Weight, %	C	O	Na	Mg	Al	Si	P	Ca	Fe
Sample 1	6.36	54.26	0.49	0.39	–	4.84	0.23	11.52	21.89
Sample 2	6.35	53.12	0.45	0.50	0.31	4.83	0.32	13.62	20.51
Sample 3	6.05	48.03	0.52	0.48	0.33	6.07	–	8.75	29.77
Max.	6.36	54.26	0.45	0.39	0.33	6.07	0.32	13.62	29.77
Min.	6.05	48.03	0.52	0.50	0.31	4.83	0.23	8.75	20.51

– Not detected.

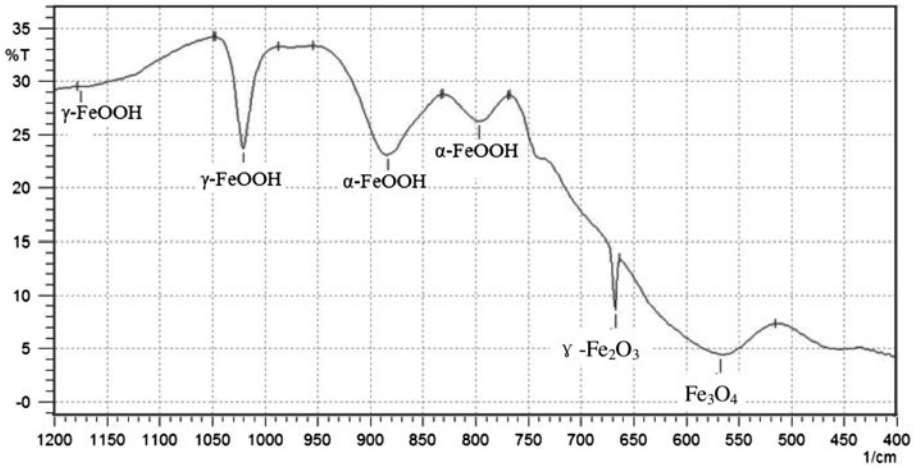

Fig. 7. The FITR patterns of the corrosion scales on carbon steel coupons.

$Fe_5HO_8{\cdot}4H_2O$ in the presence of green rust. During the transformation, $Fe_5HO_8{\cdot}4H_2O$ transferred electron on the surface by absorbing $FeOH^+$ and then formed FeOOH [39].

4. Conclusions

Carbon steel corrosion in reclaimed wastewater for cooling systems was studied. The following conclusions were obtained:

(1) Corrosion of carbon steel in reclaimed wastewater was mainly affected by Cl^-, followed by SO_4^{2-}, while the effects of NO_3^- and NH_4^+ were relatively little.
(2) Electrochemical studies revealed that the corrosion process was controlled by cathodic reaction. Corrosion rate increased at the initial stage and then decreased thereafter due to the combined action of ions and corrosion layer. The ions affected the initial corrosion of carbon steel in cooling system, while the corrosion layer hindered this effect.
(3) The corrosion layer was dense, uniform, and made up of crystalline particles. The main corrosion products were ferric hydroxides and iron oxide.
(4) Focusing on the corrosion problems in the cooling system, the concentrations of Cl^- and SO_4^{2-} should be the major pollutants to be controlled. Additionally, the corrosion process of carbon steel in reclaimed water was controlled by the catholic reaction and accompanied with the anodic reaction. So the mix corrosion inhibitors would be selected, such as PBTCA, PASP, and so on.

Acknowledgments

This research was supported by the Jiangsu Science and Technology Support Plan (BE2009604) and the National Science and Technology Major Project: Control and Management of the Polluted Water Bodies (2012ZX07301-001).

References

[1] T. Asano, F. Burton, H. Leverenz, R. Tsuchihashi, G. Tchobanoglous, Water Reuse: Issues, Technologies, and Applications, McGraw-Hill, New York, NY, 2007.
[2] G.W. Miller, Integrated concepts in water reuse: managing global water needs, Desalination 187 (2006) 65–75.
[3] B. Wijesinghe, R.B. Kaye, C.J.D. Fell, Reuse of treated sewage effluent for cooling water make up: A feasibility study and a pilot plant study, Water Sci. Technol. 33 (1996) 363–369.
[4] H.J. Gray, C.V. McGuigan, H.W. Rowland, Treated sewage serves as tower makeup, Power 117 (1973) 75–77.
[5] R. Vidic, D. Dzombak, M. Hsieh, H. Li, S. Chien, Y. Feng, I. Chowdhury, J. Monnell, Reuse of Treated Internal or External Wastewaters In the Cooling Systems of Coal-based Thermoelectric Power Plants, University of Pittsburgh, Pittsburgh, PA, 2009.
[6] Y. Zhang, D. Hou, Y.S. Li, C. Piao, Researches on the corrosion factors of the circulating cooling water system for which municipal wastewater is reused, Ind. Water Treat. 3 (2001) 1–3 (in Chinese).
[7] H. Li, M. Hsieh, S. Chien, J.D. Monnell, D.A. Dzombak, R.D. Vidic, Control of mineral scale deposition in cooling systems using secondary-treated municipal wastewater, Water Res. 45 (2011) 748–760.
[8] K.A. Selby, P.R. Puckorius, K.R. Helm, The use of reclaimed water in electric power stations and other industrial facilities, Water Air Soil Pollut. 90 (1996) 183–193.
[9] M. Hsieh, H. Li, S. Chien, J.D. Monnell, I. Chowdhury, D.A. Dzombak, R.D. Vidic, Corrosion control when using secondary treated municipal wastewater as alternative makeup water for cooling tower systems, Water Environ. Res. 82 (2010) 2346–2356.
[10] W.F. Bogaerts, A.A. Van Haute, Chloride pitting and water chemistry control in cooling or boiler circuits, Corros. Sci. 25 (1985) 1149–1161.
[11] T. Tsuru, Anodic dissolution mechanisms of metals and alloys, Mater. Sci. Eng. 146 (1991) 1–14.

[12] B. Sherar, I.M. Power, P.G. Keech, S. Mitlin, G. Southam, D. W. Shoesmith, Characterizing the effect of carbon steel exposure in sulfide containing solutions to microbially induced corrosion, Corros. Sci. 53 (2011) 955–960.
[13] Q. Bao, D. Zhang, Y. Wan, 2-Mercaptobenzothiazole doped chitosan/11-alkanethiolate acid composite coating: Dual function for copper protection, Appl. Surf. Sci. 257 (2011) 10529–10534.
[14] H.H. Uhlig, Corrosion and Corrosion Control: An Introduction to Corrosion Science and Engineering, 2nd ed., J. Wiley, New York, NY, 1971.
[15] M. Rebhun and G. Engel, Reuse of wastewater for industrial cooling systems, J. Water Pollut. Control Fed. (1988) 237–241.
[16] Y. Ma, Y. Li, F. Wang, Corrosion of low carbon steel in atmospheric environments of different chloride content, Corros. Sci. 51 (2009) 997–1006.
[17] A.E. Broo, B. Berghult, T. Hedberg, Copper corrosion in drinking water distribution systems-the influence of water quality, Corros. Sci. 39 (1997) 1119–1132.
[18] A. Elfström Broo, B. Berghult, T. Hedberg, Drinking water distribution - The effect of natural organic matter (NOM) on the corrosion of iron and copper, Water Sci. Technol. 40 (1999) 17–24.
[19] C. Campanac, L. Pineau, A. Payard, G.B. Mouysset, C. Roques, Interactions between biocide cationic agents and bacterial biofilms, Antimicrob. Agents Chemother. 46 (2002) 1469–1474.
[20] P. Melidis, M. Sanozidou, A. Mandusa, K. Ouzounis, Corrosion control by using indirect methods, Desalination 213 (2007) 152–158.
[21] S.K. Ishii, T.H. Boyer, Evaluating the secondary effects of magnetic ion exchange: Focus on corrosion potential in the distribution system, Desalination 274 (2011) 31–38.
[22] Y. Zhang, D.L. Hou, S. Yu, C. Bu, Researches on the corrosion factors of the circulating cooling water system for which municipal wastewater is reused, Ind. Water Treat. 21 (2001) 1–3 (in Chinese).
[23] I.B. Beech, J. Sunner, Biocorrosion: Towards understanding interactions between biofilms and metals, Curr. Opin. Biotechnol. 15 (2004) 181–186.
[24] Z.H. Dong, T. Liu, H.F. Liu, Influence of EPS isolated from thermophilic sulphate - Reducing bacteria on carbon steel corrosion, Biofouling 27 (2011) 487–495.
[25] B.J. Little, R.I. Ray, R.K. Pope, Relationship between corrosion and the biological sulfur cycle: A review, Corrosion 56 (2000) 433–443.
[26] H.X. Wu, Y.M. Liu, Ammonia nitrogen effect on the circulating cooling water system in the municipa1 wastewater reusing, Ind. Water Treat. 10 (2004) 30–32 (in Chinese).
[27] Y. Zhang, A. Griffin, M. Edwards, Effect of nitrification on corrosion of galvanized iron, copper, and concrete, J. Am. Water Works Assn. 102 (2010) 83–93.
[28] D. Wasser, Internal Corrosion of Water Distribution Systems, A.W.W.A. Research, Foundation/DVGW-Technologiezentrum Wasser, Karlsruhe, 1996.
[29] B. Zhou, Industrial Water Treatment Technology, Chemistry Industry Press, Beijing, 2002 (in Chinese).
[30] W.A. Khalil, A. Goonetilleke, S. Kokot, S. Carroll, Use of chemometrics methods and multicriteria decision-making for site selection for sustainable on-site sewage effluent disposal, Anal. Chim. Acta 506 (2004) 41–56.
[31] H. Castaneda, X.D. Benetton, SRB-biofilm influence in active corrosion sites formed at the steel-electrolyte interface when exposed to artificial seawater conditions, Corros. Sci. 50 (2008) 1169–1183.
[32] X. Li, S. Deng, H. Fu, G. Mu, Inhibition effect of 6-benzylaminopurine on the corrosion of cold rolled steel in H_2SO_4 solution, Corros. Sci. 51 (2009) 620–634.
[33] J. Aljourani, K. Raeissi, M.A. Golozar, Benzimidazole and its derivatives as corrosion inhibitors for mild steel in 1 M HCl solution, Corros. Sci. 51 (2009) 1836–1843.
[34] R. Johnsen, E. Bardal, Cathodic properties of different stainless steels in natural seawater, Corrosion 41 (1985) 296–302.
[35] H. Zhang, S.C. Dexter, Effect of biofilms on crevice corrosion of stainless steels in coastal seawater, Corrosion 51 (1995) 56–66.
[36] C.F. Chen, M.X. Lu, G.X. Zhao, M.L. Yan, Z.Q. Bai, Y.Q. Yang, The pitting corrosion induced by CO_2 of N80 oil steel, Chin. Soc. Corros. Prot. 23 (2003) 21–25 (in Chinese).
[37] M. Sánchez, J. Gregori, C. Alonso, J.J. García-Jareño, H. Takenouti, F. Vicente, Electrochemical impedance spectroscopy for studying passive layers on steel rebars immersed in alkaline solutions simulating concrete pores, Electrochim. Acta 52 (2007) 7634–7641.
[38] A. Rajasekar, T. Ganesh Babu, S. Karutha Pandian, S. Maruthamuthu, N. Palaniswamy, A. Rajendran, Biodegradation and corrosion behavior of manganese oxidizer Bacillus cereus ACE4 in diesel transporting pipeline, Corros. Sci. 49 (2007) 2694–2710.
[39] L. Yu, Q. Zhong, Preparation of adsorbents made from sewage sludges for adsorption of organic materials from wastewater, J. Hazard. Mater. 137 (2006) 359–366.